PHYSICAL REVIEW B **85**, 014111 (2012)

Lattice constants from semilocal density functionals with zero-point phonon correction

Pan Hao,[1,*] Yuan Fang,[1] Jianwei Sun,[1] Gábor I. Csonka,[2] Pier H. T. Philipsen,[3] and John P. Perdew[1]

[1]*Department of Physics and Engineering Physics, Tulane University, New Orleans, Louisiana 70118, USA*

[2]*Department of Inorganic and Analytical Chemistry, Budapest University of Technology and Economics, H-1521 Budapest, Hungary*

[3]*Scientific Computing and Modeling NV, Theoretical Chemistry, Vrije Universiteit, De Boelelaan 1083, 1081 HV Amsterdam, The Netherlands*

(Received 11 October 2011; revised manuscript received 26 December 2011; published 20 January 2012)

In a standard Kohn-Sham density functional calculation, the total energy of a crystal at zero temperature is evaluated for a perfect static lattice of nuclei and minimized with respect to the lattice constant. Sometimes a zero-point vibrational energy, whose anharmonicity expands the minimizing or equilibrium lattice constant, is included in the calculation or (as here) is used to correct the experimental reference value for the lattice constant to that for a static lattice. A simple model for this correction, based on the Debye and Dugdale-MacDonald approximations, requires as input only readily available parameters of the equation of state, plus the experimental Debye temperature. However, particularly because of the rough Dugdale-MacDonald estimation of Grüneisen parameters for diatomic solids, this simple model is found to overestimate the correction by about a factor of two for some solids in diamond and zinc-blende structures. Using the quasiharmonic phonon frequencies calculated from density functional perturbation theory gives a more accurate zero-point anharmonic expansion (ZPAE) correction. However, the error statistics for the lattice constants of various semilocal density functionals for the exchange–correlation energy are little changed by improving the ZPAE correction. The Perdew-Burke-Ernzerhof generalized gradient approximation (GGA) for solids and the revised Tao-Perdew-Staroverov-Scuseria (revTPSS) meta-GGA, the latter of which is implemented self-consistently here in the band-structure program BAND and applied to a test set of 58 solids, remain the most accurate of the functionals tested, with MAREs below 0.7% for the lattice constants. The most positive and most negative revTPSS relative errors tend to occur for solids for which full nonlocality (missing from revTPSS) may be important.

DOI: 10.1103/PhysRevB.85.014111 PACS number(s): 71.15.Mb, 63.20.dk, 63.20.Ry

I. INTRODUCTION

The equilibrium lattice constant of a solid[1] can be measured accurately (e.g., by x-ray diffraction) at low temperature and extrapolated to absolute zero, where it becomes a fundamental ground state property. All properties of a solid depend upon the lattice constant, and some—e.g., ferromagnetism, ferroelectricity, or epitaxy—can be very sensitive to it. Kohn-Sham density functional theory[2] (DFT) in principle predicts the ground state energy and density of electrons in the presence of a static external potential and has long been used to calculate the equation of state or energy per unit cell of a solid as a function of the lattice constant for a given crystal structure. The equilibrium lattice constant is then the one that minimizes the energy. The accuracy of the predicted lattice constant is a test of the accuracy of the approximate density functional that must be employed for the exchange–correlation energy.

The simplest calculation of the lattice constant assumes a perfect static lattice. If the nuclei were fully classical particles, they would form such a lattice at zero temperature.[3] But in quantum mechanics, all systems undergo fluctuation in their ground state. The nuclear fluctuation in a solid is crystal vibration and exists even at zero temperature. For a periodic solid, the vibration has normal modes, which are quantized as phonons.[1] Although the zero-point energy of the vibration is minor compared to the kinetic energy of the electrons and the Coulomb energy in the system, its anharmonicity (dependence of the frequency or zero-point energy on the lattice constant) can expand the equilibrium lattice constant by 1% or more for light atoms like Li and by much less for heavy atoms. Typically, as here, the uncorrected lattice constant from DFT is compared to an experimental value corrected to the static-lattice case.

DFT in the formulation of Kohn and Sham gives the ground state static-lattice energy as a functional of the electron density $n(\vec{r})$ or its up- and down-spin components:

$$E = T_S[n_\uparrow, n_\downarrow] + \int d^3r n(\vec{r})\upsilon(\vec{r}) + U[n] + E_{XC}[n_\uparrow, n_\downarrow] + V_{nn}. \quad (1)$$

The five terms on the right of Eq. (1) represent the noninteracting kinetic energy of the electrons, the Coulomb interaction between electrons and nuclei, the Hartree energy of electron–electron repulsion, the exchange–correlation energy of the electrons, and the nucleus–nucleus repulsion, respectively. The first three terms can be calculated exactly from energy-minimizing occupied orbitals for a given set of nuclear positions; the exchange–correlation energy can only be approximated in practice.

Semilocal approximations to the exchange–correlation energy are widely used for solids, because they are often nonempirical and are computationally faster than all other methods. Because of the slowly varying density in many sp-bonded solids near equilibrium, the semilocal functionals can work well,[4] although they can make larger errors for other solids in which there are important long-range van der Waals interactions or in which electrons are shared over stretched bonds.[4] In this paper, we test five nonempirical local and semilocal functionals belonging to different levels of a ladder of approximations: the local density approximation (LDA),[2,5] Perdew-Burke-Ernzerhof (PBE)[6] and Perdew-Burke-Ernzerhof for solids (PBEsol)[7] that belong to the generalized gradient approximation (GGA) level,[6,8,9]

TABLE I. The zero-point energy per atom (columns 1 and 2), the Grüneisen parameter (columns 3 and 4), and the lattice constant correction as a percentage of the experimental lattice constant using the simple model and phonon correction (columns 5 and 6, respectively).

Solid[a,b]	$3/2\hbar\omega_D$[c]	$3/2\hbar\omega_0$[d]	γ_{DM}[e]	γ_0[f]	$\frac{\Delta a_{SM}}{a_{\text{expt.}}}$(%)	$\frac{\Delta a_{\text{phonon}}}{a_{\text{expt.}}}$(%)
Li(A2) (1,2)	0.0333	0.0406	1.2755	0.9434	0.831	0.748
Na(A2) (1,2)	0.0153	0.0146	1.3223	1.5435	0.382	0.425
K(A2) (1,2)	0.0088	0.0090	1.1779	1.4180	0.210	0.259
Rb(A2) (1,2)	0.0054		0.7946		0.085	
Ca(A1) (1,4)	0.0223	0.0209	1.0250	1.2406	0.154	0.175
Sr(A1) (1,4)	0.0143	0.0103	1.2114	1.2543	0.135	0.101
Ba(A2) (1,2)	0.0107	0.0095	0.7823	0.6839	0.076	0.059
V(A2) (1,2)	0.0368	0.0325	1.3295	1.7719	0.116	0.137
Nb(A2) (1,2)	0.0267	0.0272	1.3480	1.7514	0.063	0.084
Ta(A2) (1,2)	0.0233	0.0217	2.0261	2.1602	0.072	0.072
Mo(A2) (1,2)	0.0436	0.0391	1.6008	1.8187	0.088	0.090
W(A2) (1,2)	0.0388	0.0376	1.2070	1.0957	0.050	0.044
Fe(A2) (1,2)	0.0456	0.0450	2.1346	1.8522	0.264	0.226
Rh(A1) (1,4)	0.0465	0.0367	2.1495	2.4203	0.145	0.129
Ir(A1) (1,4)	0.0407	0.0302	2.0015	2.3073	0.087	0.074
Ni(A1) (1,4)	0.0436	0.0436	1.9287	1.6726	0.220	0.191
Pd(A1) (1,4)	0.0266	0.0293	2.3443	2.4352	0.117	0.134
Pt(A1) (1,4)	0.0233	0.0251	2.1693	2.5823	0.065	0.083
Cu(A1) (1,4)	0.0333	0.0353	2.0179	1.9153	0.216	0.218
Ag(A1) (1,4)	0.0218	0.0237	2.4210	2.2937	0.154	0.158
Au(A1) (1,4)	0.0160	0.0195	2.4176	2.5853	0.068	0.089
Al(A1) (1,4)	0.0415	0.0411	1.7924	1.8695	0.305	0.316
C(A4) (2,8)	0.2162	0.1894	1.3584	0.8113	0.624	0.327
Si(A4) (2,8)	0.0625	0.0610	1.6134	0.9063	0.271	0.149
Ge(A4) (2,8)	0.0363	0.0338	1.9000	1.2914	0.215	0.136
Sn(A4) (2,8)	0.0194	0.0215	2.0703	1.4068	0.119	0.089
Pb(A1) (1,4)	0.0102	0.0099	2.0798	2.4276	0.078	0.088
LiF(B1) (2,8)	0.0710	0.0681	1.6392	1.3975	1.104	0.903
LiCl(B1) (2,8)	0.0409	0.0339	1.8958	2.1750	0.703	0.668
NaF(B1) (2,8)	0.0477	0.0526	1.7637	1.8814	0.714	0.840
NaCl(B1) (2,8)	0.0311	0.0298	1.8997	1.9916	0.542	0.545
MgO(B1) (2,8)	0.0917	0.0762	1.5496	1.6760	0.494	0.444
MgS(B1) (2,8)	0.0630	0.0399	1.3654	1.7913	0.326	0.271
CaO(B1) (2,8)	0.0628	0.0894	1.7341	1.5286	0.365	0.458
TiC(B1) (2,8)	0.0911	0.0840	1.6262	1.4557	0.335	0.276
TiN(B1) (2,8)	0.0734	0.0823	1.6270	1.8301	0.242	0.305
ZrC(B1) (2,8)	0.0679	0.0691	1.4781	1.4324	0.200	0.197
ZrN(B1) (2,8)	0.0679	0.0622	1.6413	1.7809	0.206	0.205
HfC(B1) (2,8)	0.0536		1.5300		0.145	
HfN(B1) (2,8)	0.0590		1.3706		0.159	
VC(B1) (2,8)	0.0590	0.0783	1.5643	1.9402	0.181	0.297
VN(B1) (2,8)	0.0732		1.6391		0.269	
NbC(B1) (2,8)	0.0738	0.0714	1.6240	1.7236	0.191	0.196
NbN(B1) (2,8)	0.0708		1.6364		0.203	
FeAl(B2) (2,2)	0.0498	0.0520	1.5321	1.6112	0.248	0.273
CoAl(B2) (2,2)	0.0485	0.0539	1.5767	1.5645	0.215	0.237
NiAl(B2) (2,2)	0.0390	0.0455	1.6301	1.8242	0.170	0.222
BN(B3) (2,8)	0.1648	0.1718	1.3297	0.8454	0.536	0.355
BP(B3) (2,8)	0.0955	0.1003	1.4024	0.8298	0.403	0.250
BAs(B3) (2,8)	0.0776	0.0818	1.5245	1.1868	0.336	0.276
AlP(B3) (2,8)	0.0570	0.0538	1.4979	0.9866	0.301	0.187
AlAs(B3) (2,8)	0.0283	0.0435	1.6012	1.1949	0.144	0.166
GaN(B3) (2,8)	0.0582	0.0778	1.7133	0.9759	0.235	0.179
GaP(B3) (2,8)	0.0431	0.0344	1.8919	1.1896	0.247	0.124
GaAs(B3) (2,8)	0.0333	0.0322	1.7991	1.1947	0.188	0.121
InP(B3) (2,8)	0.0311	0.0377	1.8653	1.2787	0.173	0.144
InAs(B3) (2,8)	0.0239	0.0266	1.9688	1.1212	0.156	0.099
SiC(B3) (2,8)	0.1194	0.1084	1.4656	0.9086	0.402	0.226

[a]The Strukturbericht symbols (in parentheses) are used for the structures as follows: A1, fcc; A2, bcc; A4, diamond; B1, rocksalt; B2, CsCl; B3, zinc blende.

[b]The two numbers in parentheses are the number of atoms per primitive cell followed by the number of atoms per conventional cubic cell.

[c]From the simple model. The unit is electron volts.

[d]From the phonon model. The unit is electron volts.

[e]From the Dugdale-MacDonald model.

[f]From the curve of phonon zero-point energy versus lattice constant.

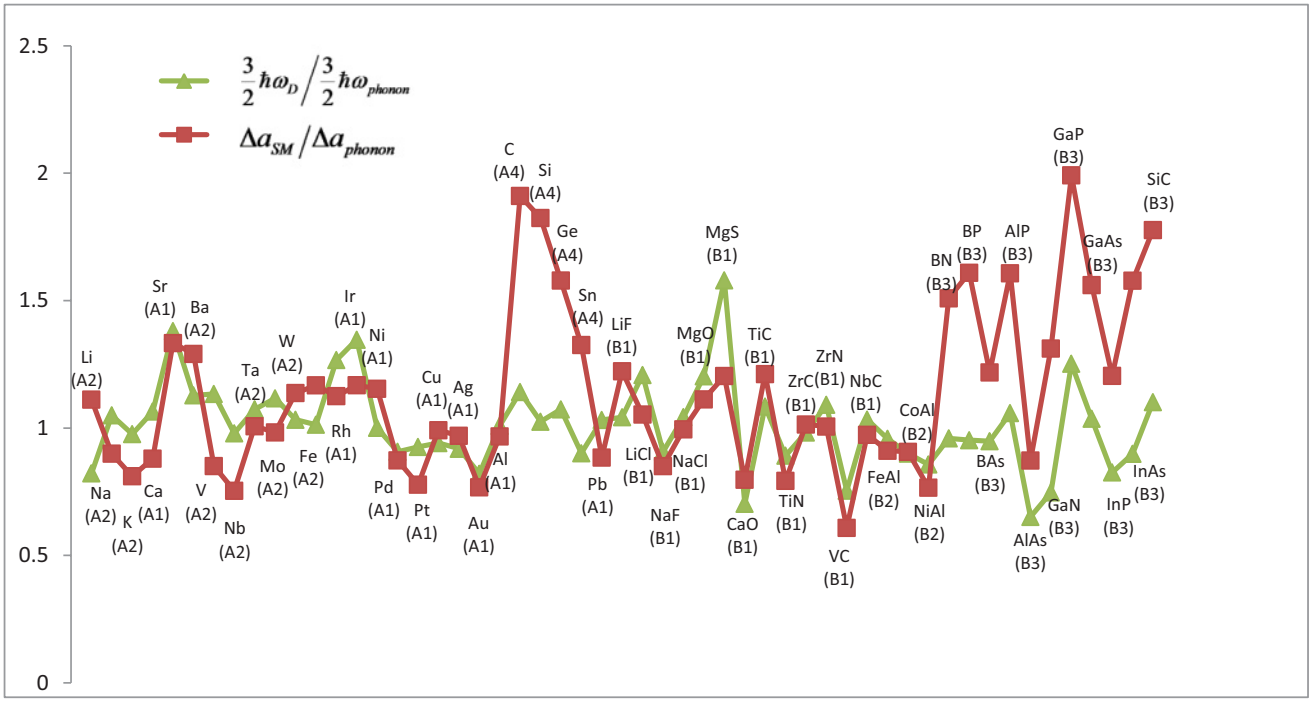

FIG. 1. (Color online) The light gray (green) line is the ratio of the zero-point energy approximated by the Debye model to that computed from the phonon average frequency. The dark gray (red) line is the ratio of the lattice constant correction ($\boldsymbol{\Delta a}$) calculated by the simple model to that calculated by the phonon model.

and Tao-Perdew-Staroverov-Scuseria (TPSS)[10] and revised Tao-Perdew-Staroverov-Scuseria (revTPSS)[11] that belong to the meta-GGA level. The early and simple local spin density approximation (LSDA) gives lattice constants that are too short for solids and overestimated atomization energies. The PBE GGA predicts reasonable but too-long lattice constants and improves atomization energies. The TPSS meta-GGA predicts lattice constants only a little smaller than those of PBE but gives better atomization energies for molecules than PBE does. While PBE is a general-purpose GGA for atoms, molecules, and solids, the PBEsol[7,12,13] GGA has a diminished gradient dependence[14] designed specifically for solids and solid surfaces near equilibrium. The revTPSS meta-GGA, which takes insights from the PBEsol construction, gives lattice constants as accurate as those of PBEsol while keeping the atomization energies as accurate as those of TPSS.

A simple model for the contribution of zero-point anharmonic expansion (ZPAE) to the lattice constant of a solid was proposed in Ref. 15 and used in Refs. 16–20 to test various density functionals. Ref. 18 introduced the large test set of 58 solids, which we use here. The more accurate but more computationally demanding phonon model for zero-point anharmonic contribution has been used, e.g., in Refs. 21 and 22. Ref. 22 compared the simple and phonon models for a test set about half the size of ours, including some solids in diamond and zinc-blende structures, and reached conclusions similar to but less analyzed than those we reach here. In particular, we show that the simple model is reasonably accurate except in diamond and zinc-blende structures, where its error arises mainly from the Dugdale-MacDonald model for the Grüneisen parameter and less from the Debye model for vibrational energy. Our work was well under way before we learned of Ref. 22.

References 17–19 employed a non-self-consistent implementation of the meta-GGAs. Ref. 23 implemented the revTPSS meta-GGA self-consistently in Vienna *ab initio* simulation package (VASP) code, and Ref. 20 applied revTPSS to a carbon monoxide molecule on transition-metal surfaces. Here, we implement revTPSS self-consistently in the solid state band-structure code BAND.

II. THE ZPAE CORRECTION: FROM A SIMPLE TO A PHONON MODEL

The widely used ZPAE method gives the lattice constant correction to a DFT calculation at zero temperature. In the simple model, the zero-point energy is given by the Debye model,[1] and the volume expansion of it is given by the Dugdale-MacDonald model.[24] The inputs of the simple model are the Debye temperature, the bulk modulus, and the first derivative of the bulk modulus with pressure. The first two quantities can be found from accurate experimental values[18] for the low-temperature specific heat and compressibility. For the first derivative of the bulk modulus, which is not given so accurately by experiment, we use theoretical TPSS values, as was done in Ref. 16.

The derivation of the simple model is given with telegraphic brevity in Appendix A of Ref. 15. Here, we show how to derive the simple model correction, starting from Eq. A1 of that appendix, where all quantities are "per atom." We begin with the total energy per atom

$$\varepsilon(v) = \varepsilon^0(v) + \frac{3}{2}\hbar\omega(v), \tag{2}$$

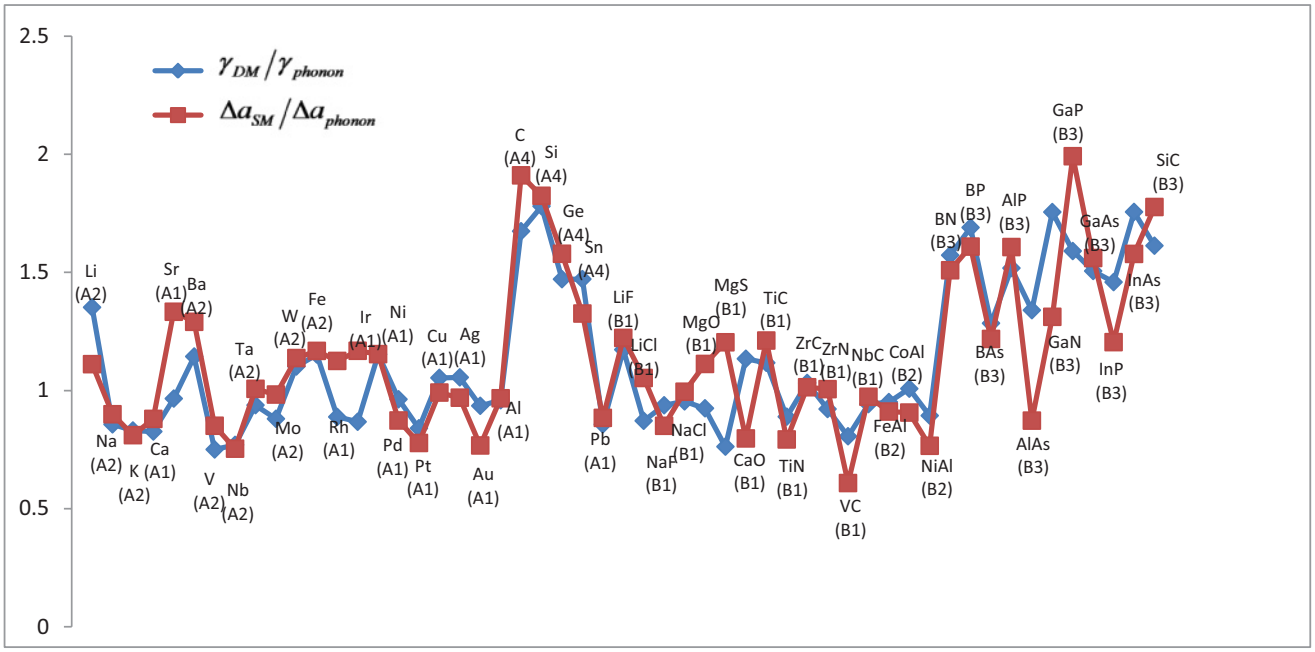

FIG. 2. (Color online) The light gray (blue) line is the ratio of the Grüneisen parameter approximated by the Dugdale-MacDonald model to that approximated by the phonon model. The dark gray (red) line is the ratio of the lattice constant correction ($\mathbf{\Delta}\boldsymbol{a}$) calculated by the simple model to that calculated by the phonon model. Note the similarity of the two curves, which shows that most of the error of the simple model arises from the Dugdale-MacDonald approximation.

where v is the volume per atom, which for the solids we consider is equal to $a^3/2$ for the body-centered cubic (bcc) and CsCl structures, $a^3/4$ for the face-centered cubic (fcc) structure, and $a^3/8$ for the rocksalt, diamond, and zinc-blende structures. Here, a is the cube-side lattice constant, $\varepsilon^0(v)$ is the ground state energy given by a DFT calculation without the zero-point energy correction, and $\frac{3}{2}\hbar\omega$ is the phonon zero-point energy per atom, where ω is an average phonon frequency.

The Taylor expansion to second order of $\varepsilon(v)$ around v_0 is

$$\varepsilon(v) = \varepsilon^0(v_0) + \frac{\alpha}{2}(v - v_0)^2 + \frac{3}{2}\hbar\omega(v_0) + \beta(v - v_0), \quad (3)$$

where v_0 is the equilibrium volume calculated from the DFT method. In Eq. (3), the first two terms on the right arise from the DFT calculation, and the second two terms arise from the zero-point vibrational energy. Here, $\alpha = \frac{d^2\varepsilon^0}{dv^2}|_{v_0} = \frac{B_0}{v_0}$, where B_0 is the equilibrium bulk modulus. For the zero-point energy, the average frequency ω is nearly linear in volume around the equilibrium volume, and $\beta = \frac{3}{2}\hbar\frac{d\omega}{dv}|_{v_0}$. Since the Grüneisen parameter at equilibrium is $\gamma_0(v) = -\frac{v}{\omega}\frac{d\omega}{dv}|_{v_0}$, we find $\beta = -\frac{3}{2}\gamma_0\frac{\hbar\omega_0}{v_0}$.

Because the derivative of ε with respect to v is equal to zero at the real equilibrium position, from Eq. (3) we have $\alpha(v - v_0) + \beta = 0$. So the correction to the DFT-calculated volume is

$$\Delta v = (v - v_0) = -\frac{\beta}{\alpha} = \frac{3}{2}\gamma_0\frac{\hbar\omega_0}{B_0}. \quad (4)$$

So far, the volume correction is derived without serious approximation. When we choose the Grüneisen parameter as $\gamma_0(v) \approx \frac{1}{2}(B_1 - 1)$ from the Dugdale-MacDonald model[24] (where B_1 is the pressure derivative of the bulk modulus at equilibrium) and combine it with the Debye approximation $\hbar\omega = \frac{3}{4}k_B\Theta_D$ (where Θ_D is the Debye temperature), we get the simple model

$$\frac{\Delta v}{v_0} = \frac{3\Delta a}{a_0} = \frac{9}{16}(B_1 - 1)\frac{k_B\Theta_D}{B_0 v_0}. \quad (5)$$

The underlying picture of the Debye and Dugdale-MacDonald approximations is a crystal with one atom per primitive cell. The approximations may work, but less reliably, when there is more than one atom per cell. The Dugdale-MacDonald model has a correct limit: The anharmonic effects vanish for a harmonic crystal ($B_1 = 1$).

To see how well the simple model works, we compare the simple model to our phonon model. In the phonon model, the zero-point energy is calculated from the average frequency of lattice vibration using Quantum Espresso (QE) code instead

TABLE II. Test of revTPSS self-consistency employing the bond lengths (in angstroms) of the Li, N, and Ca dimers.

Molecule	Energy[a]	Grad = 0[b]	Difference
Li_2	2.75687	2.75671	−0.00016
N_2	1.10069	1.10069	−0.00005
Ca_2	4.10702	4.10675	−0.00026

[a]"Energy" means calculating a revTPSS total energy for bond lengths separated by 0.01 bohr, fitting the result, and minimizing the fitted energy.

[b]"Grad = 0" means optimizing the geometry until the forces are less than 10^{-8} hartree per bohr.

TABLE III. Theoretical lattice constants (in angstroms) calculated from BAND code using LSDA, PBE, PBEsol, TPSS, and revTPSS functionals. The revTPSS density is used for all calculations. The experimental lattice constants are corrected for ZPAE.

Solid	LSDA BAND	PBE BAND	PBEsol BAND	TPSS BAND	revTPSS BAND	Expt. − Δa
Li	3.368	3.429	3.429	3.446	3.434	3.451
Na	4.051	4.197	4.174	4.249	4.222	4.207
K	5.050	5.281	5.220	5.369	5.325	5.211
Rb[a]	5.374	5.665	5.571	5.768	5.716	5.580
Ca	5.321	5.521	5.449	5.540	5.520	5.555
Sr	5.779	6.013	5.911	6.023	6.001	6.042
Ba	4.732	5.022	4.874	5.002	4.978	5.004
V	2.924	2.997	2.958	2.975	2.968	3.024
Nb	3.246	3.310	3.272	3.294	3.284	3.293
Ta	3.298	3.347	3.320	3.329	3.317	3.299
Mo	3.110	3.161	3.130	3.147	3.137	3.141
W	3.122	3.170	3.141	3.153	3.139	3.161
Fe	2.749	2.834	2.788	2.804	2.793	2.855
Rh	3.749	3.827	3.777	3.800	3.780	3.793
Ir	3.812	3.872	3.832	3.851	3.829	3.832
Ni	3.419	3.517	3.461	3.475	3.455	3.509
Pd	3.832	3.932	3.869	3.887	3.862	3.876
Pt	3.895	3.971	3.920	3.943	3.916	3.913
Cu	3.518	3.630	3.565	3.577	3.551	3.595
Ag	4.001	4.150	4.055	4.086	4.051	4.063
Au	4.039	4.147	4.074	4.103	4.069	4.061
Al	3.982	4.037	4.014	4.011	4.008	4.019
C	3.532	3.571	3.553	3.569	3.559	3.555
Si	5.402	5.468	5.432	5.452	5.438	5.422
Ge	5.624	5.764	5.679	5.723	5.680	5.644
Sn	6.475	6.659	6.543	6.612	6.560	6.476
Pb	4.882	5.040	4.935	4.981	4.939	4.912
LiF	3.915	4.064	4.005	4.031	4.013	3.974
LiCl	4.972	5.147	5.063	5.093	5.085	5.072
NaF	4.502	4.700	4.630	4.706	4.675	4.570
NaCl	5.466	5.695	5.606	5.705	5.671	5.565
MgO	4.162	4.255	4.216	4.237	4.233	4.188
MgS	5.127	5.228	5.184	5.228	5.222	5.188
CaO	4.709	4.832	4.769	4.809	4.808	4.781
TiC	4.260	4.332	4.293	4.328	4.316	4.318
TiN	4.171	4.247	4.204	4.239	4.231	4.226
ZrC	4.639	4.708	4.668	4.707	4.694	4.687
ZrN	4.524	4.594	4.552	4.588	4.580	4.576
HfC[a]	4.571	4.655	4.609	4.646	4.624	4.631
HfN[a]	4.470	4.553	4.506	4.540	4.524	4.513
VC	4.087	4.154	4.116	4.146	4.132	4.148
VN[a]	4.041	4.116	4.073	4.108	4.097	4.130
NbC	4.425	4.484	4.449	4.481	4.465	4.461
NbN[a]	4.355	4.422	4.381	4.417	4.404	4.383
FeAl	2.811	2.868	2.840	2.850	2.842	2.881
CoAl	2.793	2.851	2.823	2.832	2.822	2.854
NiAl	2.832	2.892	2.862	2.872	2.862	2.881
BN	3.581	3.624	3.605	3.621	3.615	3.594
BP	4.491	4.548	4.520	4.544	4.529	4.527
BAs	4.733	4.809	4.768	4.799	4.774	4.764
AlP	5.433	5.504	5.468	5.492	5.482	5.450
AlAs	5.631	5.728	5.676	5.702	5.682	5.649
GaN	4.457	4.549	4.499	4.532	4.518	4.523
GaP	5.392	5.506	5.439	5.488	5.460	5.441
GaAs	5.607	5.751	5.664	5.716	5.675	5.641
InP	5.829	5.963	5.882	5.949	5.918	5.858

TABLE III. (*Continued*)

Solid	LSDA BAND	PBE BAND	PBEsol BAND	TPSS BAND	revTPSS BAND	Expt. − Δa
InAs	6.026	6.188	6.089	6.157	6.113	6.048
SiC	4.329	4.378	4.356	4.366	4.357	4.348
ME[b]	**− 0.064**	**0.043**	**−0.010**	**0.030**	**0.010**	
MAE[b]	**0.064**	**0.049**	**0.028**	**0.040**	**0.030**	
MRE[b] (%)	**−1.478**	**0.894**	**−0.295**	**0.549**	**0.115**	
MARE[b] (%)	**1.478**	**1.048**	**0.641**	**0.856**	**0.675**	

[a]For the solids Rb, HfC, HfN, VN, and NbN, the simple model is used; for all other solids, phonon correction is used.
[b]Error statistics are in boldface.

of the Debye model. It is $\varepsilon_{vib} = \frac{\int_0^\infty \frac{3}{2}\hbar\, g(\omega)d\omega}{\int_0^\infty g(\omega)d\omega}$, where $g(\omega)$ is the density of phonon states. $\int_0^\infty g(\omega)d\omega$ is the number of modes of vibration per primitive cell. For a monatomic crystal, $\int_0^\infty g(\omega)d\omega = 3$; for a diatomic structure, $\int_0^\infty g(\omega)d\omega = 6$.

Also, we can calculate the Grüneisen parameter at equilibrium $\gamma_0(v)$ from its definition using the curve of zero-point energy versus lattice constant. $\gamma_0(v) = -\frac{1}{3}\frac{a_0}{\varepsilon_{vib0}}\frac{d\varepsilon_{vib}}{da}$, where a_0 is the equilibrium lattice constant calculated from the DFT method and ε_{vib0} is the zero-point energy at a_0. $\frac{d\varepsilon_{vib}}{da}$ can be evaluated around the equilibrium lattice constant.

III. RESULTS AND DISCUSSION

A. Calculation of the zero-point phonon correction

A set of 58 cubic solids[18] was considered (Table I). The phonon zero-point energy was calculated as a function of the lattice constant. The computations were realized using QE code.[25] The PBE functional was used in our phonon calculation, with PBE pseudopotentials.[26] QE code uses density functional perturbation theory[27] to calculate the interatomic force constants from first principles, which leads to the phonon frequencies. The first Brillouin zone was sampled with the 12 × 12 × 12 k-mesh for most solids. In addition, 6 × 6 × 6 q-points were used for calculating the dynamic matrix, which gives the phonon frequencies at a specified q-point in the Brillouin zone. Then the density of phonon states is calculated from a 15 × 15 × 15 mesh, which is interpolated from the 6 × 6 × 6 q-points.

The QE code uses a plane-wave basis with pseudopotentials. For the elements Rb and Hf, the pseudopotentials are not provided on the QE Web site, so we do not calculate the phonon zero-point energy of Rb, HfC, and HfN, which are in our set of solids. For solid VN and NbN, the rocksalt phase is not stable at zero temperature,[28] and for them we found nonpositive phonon frequencies in our calculation, which confirms that instability. So we do not report phonon values for VN and NbN either.

In Table I, we present the zero-point energy, Grüneisen parameter, and lattice constant correction using the simple model and the phonon model. Experimental Debye temperature, lattice constants, and bulk moduli were used (from Ref. 18), which we list in our supplementary material.[29] The pressure derivative of the bulk modulus was calculated from the TPSS functional.

In Figs. 1 and 2, we show the ratio of the zero-point energy, the ratio of the Grüneisen parameter, and the ratio of the lattice constant correction found from the simple model to that found from the phonon model. From Fig. 1, we see that the zero-point energy approximated by the Debye model is reasonably accurate. For the monatomic crystal (one atom per primitive cell: A1 and A2), the ratio of the zero-point energy is on average bigger than 1. Except for Na and Au, which have ratios smaller than 0.9, the ratios for the other monatomic solids are all above 0.9. This is because the Debye model uses a linear approximation for the dispersion curve. However, the real dispersion curve at a large wavevector in a monatomic solid has smaller frequencies than those of the Debye model, which means that the zero-point energy is overestimated by the Debye model. For a diatomic crystal (two atoms per primitive cell: A4 and B1–B3), the ratio of the zero-point energy is smaller than 1 on average. Except for LiF, MgO, MgS, and GaP, which have ratios larger than 1.2, the ratios are all under 1.2 and many are under 1.0. For a crystal with two atoms per unit cell, the Debye model continues to use a linear (in the extended zone scheme) extrapolation of the small-wavevector average acoustic dispersion, even for the optical modes. But the optical modes might be better approximated by an Einstein model, in which frequency is independent of wavevector. Thus, the Debye model tends to underestimate the optical phonon zero-point energy when the actual frequency gap between optical and acoustic modes is large and to overestimate it when this gap is small (as it is for LiF, MgO, MgS, and GaP).

In Fig. 2, the Grüneisen parameter ratio also fluctuates around and close to 1, except in the A4 and B3 structures. For the solids of A4 and B3 structures, the Grüneisen parameter given by the Dugdale-MacDonald model is at least ∼50% bigger than that given by the phonon model—and sometimes more. Because of that, the lattice constant correction given by the simple model is overestimated for solids of the A4 and B3 structures. It appears that covalent-bonding non-close-packed structures do not follow the Dugdale-MacDonald model.

B. Calculation of the lattice constants

We modified the current version of BAND,[30–32] which implements revTPSS only non-self-consistently, to implement it self-consistently. For revTPSS, the exchange–correlation energy involves the kinetic energy density $\tau(\vec{r})$, which is not an explicit functional of the density $n(\vec{r})$. So the exchange–correlation potential, $v_{xc}(\vec{r}) = \delta E_{xc}/\delta n(\vec{r})$, is not calculated directly. The partial integration method[33] is used for calculating the matrix elements of the exchange–correlation potential. All orbitals are treated numerically in BAND. We derived the partial derivatives for the revTPSS functional and tested their

TABLE IV. Relative errors (in percent) in lattice constants with respect to the ZPAE-corrected experimental values, ordered from the most positive value to the least positive value of revTPSS.

	Type of solid	LSDA	PBE	PBEsol	TPSS	revTPSS
Rb	SM	−3.70	1.52	−0.16	3.37	2.44
NaF	II	−1.50	2.84	1.31	2.98	2.29
K	SM	−3.09	1.34	0.17	3.02	2.17
NaCl	II	−1.76	2.35	0.74	2.52	1.92
Sn	SC	−0.01	2.83	1.03	2.09	1.29
InAs	SC	−0.37	2.32	0.67	1.80	1.08
MgO	II	−0.63	1.58	0.66	1.17	1.06
InP	SC	−0.48	1.80	0.42	1.57	1.04
LiF	II	−1.47	2.26	0.79	1.45	0.98
MgS	II	−1.18	0.78	−0.08	0.76	0.65
Ge	SC	−0.36	2.12	0.61	1.40	0.63
GaAs	SC	−0.61	1.95	0.41	1.33	0.59
AlP	SC	−0.31	1.00	0.34	0.77	0.59
BN	SC	−0.37	0.82	0.31	0.76	0.59
AlAs	SC	−0.31	1.40	0.48	0.95	0.58
Ta	TM	−0.03	1.48	0.65	0.91	0.57
CaO	II	−1.52	1.06	−0.25	0.59	0.56
Pb	SM	−0.60	2.61	0.47	1.41	0.56
NbN	II	−0.64	0.88	−0.06	0.77	0.49
Na	SM	−3.72	−0.25	−0.78	0.99	0.36
GaP	SC	−0.91	1.20	−0.04	0.85	0.35
Si	SC	−0.37	0.85	0.19	0.56	0.29
LiCl	II	−1.97	1.48	−0.18	0.42	0.25
HfN	II	−0.95	0.90	−0.15	0.60	0.24
BAs	SC	−0.64	0.96	0.09	0.73	0.22
SiC	SC	−0.44	0.69	0.18	0.41	0.21
Au	TM	−0.56	2.10	0.32	1.03	0.20
ZrC	II	−1.01	0.46	−0.40	0.44	0.16
TiN	II	−1.30	0.49	−0.52	0.29	0.11
C	SC	−0.66	0.44	−0.06	0.37	0.10
NbC	II	−0.81	0.50	−0.28	0.44	0.10
ZrN	II	−1.13	0.41	−0.51	0.28	0.09
Pt	TM	−0.45	1.50	0.18	0.78	0.09
BP	SC	−0.78	0.46	−0.15	0.39	0.05
TiC	II	−1.34	0.32	−0.59	0.23	−0.04
Ir	TM	−0.53	1.04	−0.01	0.49	−0.09
GaN	SC	−1.45	0.57	−0.53	0.21	−0.12
Mo	TM	−0.98	0.63	−0.37	0.20	−0.15
HfC	II	−1.30	0.51	−0.48	0.32	−0.15
Al	SM	−0.94	0.45	−0.14	−0.21	−0.27
Nb	TM	−1.44	0.52	−0.65	0.03	−0.29
Ag	TM	−1.52	2.15	−0.18	0.57	−0.29
Rh	TM	−1.15	0.91	−0.42	0.19	−0.35
Pd	TM	−1.14	1.45	−0.17	0.29	−0.36
VC	II	−1.47	0.15	−0.77	−0.03	−0.39
Li	SM	−2.42	−0.63	−0.62	−0.15	−0.49
Ba	SM	−5.45	0.36	−2.61	−0.05	−0.52
Ca	SM	−4.21	−0.61	−1.92	−0.28	−0.63
NiAl	AM	−1.69	0.40	−0.63	−0.30	−0.65
W	TM	−1.23	0.31	−0.63	−0.25	−0.67
Sr	SM	−4.36	−0.47	−2.17	−0.32	−0.68
VN	II	−2.15	−0.33	−1.38	−0.54	−0.81
CoAl	AM	−2.14	−0.11	−1.11	−0.79	−1.12
Cu	TM	−2.16	0.98	−0.85	−0.51	−1.23
FeAl	AM	−2.43	−0.45	−1.42	−1.07	−1.37
Ni	TM	−2.57	0.21	−1.37	−0.99	−1.55
V	TM	−3.30	−0.89	−2.17	−1.63	−1.86
Fe	TM	−3.70	−0.72	−2.35	−1.78	−2.15

SM, simple metal; TM, transition metal; II, ionic insulator; SC, semiconductor (A4 or B3 structures); AM, alloy metal.

TABLE V. Error statistics for the revTPSS lattice constant, compared with the corrected experimental lattice constant using two corrections, for the solids listed in Table I, excluding Rb, HfC, HfN, VN, and NbN for the phonon model.

	Simple model	Phonon model
ME	0.011	0.009
MAE	0.031	0.029
MRE (%)	0.133	0.084
MARE (%)	0.705	0.661

correctness by numerically differentiating the energy density with respect to those independent variables, including spin densities, gradients, and kinetic energy density. Relativistic effects are included in the zero-order regular approximation.

Lattice constants and bond lengths can be computed two ways: by minimizing the total energy and by zeroing out the Hellmann-Feynman forces and stresses. The results of the second approach are more sensitive to the orbitals than those of the first. The results are expected to agree only at self-consistency, so the agreement shown in Table II is a good test of self-consistency.

The BAND program uses a mixed Slater-type and numerical-type orbital basis set. In our lattice constant calculation, the quadruple zeta plus quadrupole polarization basis set is used, which is the biggest basis set in BAND code. The largest number of k-points (parameter 7) is used for solving the Kohn-Sham equations. There are 84 k-points for bcc and 196 k-points for fcc in the irreducible wedge. The lattice constants are calculated by fitting the energy curve using the stabilized jellium equation of state.[15] The functionals LSDA, PBE, PBEsol, and TPSS are evaluated with revTPSS orbitals.

In Table III, the experimental lattice constants are corrected for ZPAE. Phonon model correction is used when available. For the solids Rb, HfC, HfN, VN, and NbN, as discussed earlier, the simple model is used. The theoretical lattice constants calculated by various functionals are compared to the experimental lattice constants corrected to the static-lattice case. The mean error (ME), the mean absolute error (MAE), the mean relative error (MRE, in percent), and the mean absolute relative error (MARE, in percent) are given for each functional.

From Table III, we can clearly see that the ME, MAE, MRE, and MARE are all reduced from LDA to PBE GGA and then further reduced to the higher-level TPSS meta-GGA and revTPSS meta-GGA. PBEsol gives lattice constants as good as revTPSS. TPSS and PBE have similar statistical errors, although TPSS is slightly better than PBE. LDA underestimates the lattice constants for nearly all solids, as expected.

Table IV shows the relative errors of the lattice constants, which are always negative for LSDA but not for the other functionals. When the relative errors of revTPSS are ordered from most positive to most negative, as in Table IV, several trends emerge: (1) The most positive errors tend to occur for ionic solids with large polarizable negative ions and for heavy alkali metals with large ionic cores, where the long-range van der Waals attraction missing in revTPSS should reduce the error.[34] (2) The most negative errors occur for the 3d transition

TABLE VI. Lattice constants (in angstroms) calculated from BAND and VASP code in revTPSS, self-consistently and from the LDA density. The difference between them is presented as a possible measure of the self-consistency effect, which is expected to be largest in soft solids like these with BAND but not with VASP.

Functional Density	revTPSS revTPSS	revTPSS LDA	Difference BAND	revTPSS revTPSS	revTPSS LDA	Difference VASP
Ca	5.516	5.509	0.007	5.504	5.504	0.000
Rb	5.716	5.692	0.024	5.712	5.709	0.003
Sr	5.995	5.976	0.019	6.007	6.003	0.004
Ba	4.977	4.961	0.016	4.986	4.984	0.002

metals, where the localized but overlapped 3*d* orbitals produce a density very different from the atomic and slowly varying paradigms of the meta-GGA form. The 3*d* metals may require a non–van der Waals kind of full nonlocality also missing in revTPSS. Indeed, the relative error becomes less negative from 3*d* to 4*d* to 5*d* as the *d* orbitals become more diffuse.

In Table V, we show the ZPAE effect on the revTPSS lattice constants. The revTPSS lattice constants are compared with the corrected experimental lattice constant. For the phonon model correction, all statistical errors (ME, MAE, MRE, and MARE) are smaller than for the simple model correction.

In our calculation, self-consistent revTPSS meta-GGA is used. Self-consistent meta-GGA is more time consuming than self-consistent LDA, especially for an all-electron calculation as in BAND code. Sometimes, a non-self-consistent calculation is effective and computationally necessary. We define the self-consistency effect on the lattice constant in the following way: For a given energy functional, minimize energy versus lattice constant using the self-consistent density for that functional and then the density for another functional, e.g., LDA, and see how much the lattice constant differs. The self-consistency effect for the PBE GGA is very small, on the order of 0.001 −0.002 Å, even for soft solids like Ca, Sr, Ba, and Rb. So we expect the self-consistency effect also to be small for the revTPSS meta-GGA. For most of our solids, we can confirm this expectation, but we cannot do so for the soft solids. The self-consistency effects for the soft solids are shown in Table VI. We doubt whether these effects are real and suspect that they are simply a consequence of numerical error of revTPSS in BAND. We have not found such large revTPSS self-consistency effects with VASP. Perhaps they are only a reflection of the additional numerical errors that can arise in an all-electron code like BAND when the curve of total energy versus lattice constant is very flat. In any case, self-consistency is still important for the determination of bond lengths, bond angles, and lattice constants via Hellmann-Feynman forces and stresses, etc.

TABLE VII. The interlayer equilibrium lattice constant (in angstroms) of graphite, calculated from BAND and VASP.

Functionals	LDA	PBE	PBEsol	TPSS	revTPSS	Expt.
c (BAND)	6.7	8.7	7.4	8.8	8.8	6.71
c (VASP)	6.7	8.8	7.4	10.0	10.1	6.71

To check the performance of these functionals in a dispersion-dominated interaction system, we show the lattice constants of graphite in Table VII. The in-plane lattice constant is fixed at the experimental value 2.464 Å, and a search is made for the equilibrium interlayer distance $c/2$, where c is the lattice constant. Due to its tendency of underestimate lattice constants, which compensates for the absence of long-range dispersion in graphite, LDA spuriously predicts the most precise lattice constant. As expected, PBE yields a lattice constant that is too large, whereas PBEsol puts the lattice constant between that of LDA and that of PBE. TPSS barely binds graphite, with the minimum at 10.0 Å on VASP code, which is ∼5 Å smaller than that given in Ref. 18, and 8.8 Å on BAND code. This is probably because the TPSS calculations of Ref. 18 were non-self-consistent and the binding curve of TPSS is very flat. revTPSS performs similarly to TPSS, showing that both are unable to capture the long-range part of the dispersion or van der Waals interaction.

IV. CONCLUSIONS

In this work, the revTPSS meta-GGA is implemented self-consistently in BAND code. The lattice constants of 58 solids are calculated using the density functionals LSDA, PBE, PBEsol, TPSS, and revTPSS. LSDA makes the largest errors for solids, which makes its excellent performance for the bond lengths of diatomic molecules[35] all the more surprising. The revTPSS meta-GGA predicts the lattice constant, as well as the PBEsol GGA, and does so better than the other functionals tested. The largest positive or negative relative errors of the revTPSS lattice constants tend to occur in those solids in which some full nonlocality, absent in revTPSS, might be expected (Sec. III). Overall, revTPSS appears to be the best of the semilocal functionals tested here, since it also produces generally the most accurate atomization energies of molecules,[11] desorption energies of molecules from metal surfaces,[20] and surface energies of metals.[11,20]

The experimental lattice constant is corrected for ZPAE in two ways. The simple model gives reasonable results for most solids. However, it overestimates the correction by about a factor of two for diamond and zinc-blende structures. This simple model is based on the Debye model for vibrational energy and the Dugdale-MacDonald model for the Grüneisen parameter. The underlying picture is thus that of a solid with one atom per primitive cell. The simple model can also work, but does so unreliably, for a solid with two atoms per unit cell; it fails for the covalent diamond and zinc-blende structures,

where the Dugdale-MacDonald model is responsible for most of the failure. Diamond and zinc blende are open, covalent structures and are similar to each other. The phonon model in principle improves the zero-point energy and the Grüneisen parameter from those of the simple model. Compared to the simple model, the phonon model gives similar error statistics for lattice constants but requires more computational time, because the phonon calculation is expensive. However, the phonon model gives the more accurate zero-point energy correction, and we favor it as the benchmark ZPAE lattice constant correction. Moreover, the simple model requires a value for B_1, which is uncertain from experiment and even from calculation.

When phonon model corrections are unavailable, simple model corrections remain useful. However, greater accuracy can be achieved by empirically scaling the extreme right-hand side of Eq. (5) by a factor of 0.66 for diamond and zinc-blende structures only. This factor zeros out the MRE of the simple model for the solids in our data set with these two structures.

Although thermal expansion due to phonon excitation is not our interest here, it can be addressed by the simple and phonon models.

ACKNOWLEDGMENTS

This material is based in part upon work by J.P.P. supported by the National Science Foundation (NSF) under NSF Cooperative Agreement No. EPS-1003897, with support from the Louisiana Board of Regents. J.P.P., P.H., Y.F., and J.S. acknowledge support from the NSF under Grant No. DMR-0854769. P.H. acknowledges a Louisiana Optical Network Institute (LONI) Fellowship. The computations were made with the support of LONI and the Center for Computational Sciences at Tulane University.

*adehaopan@gmail.com

[1] N. W. Ashcroft and N. D. Mermin, *Solid State Physics* (Saunders College, Fort Worth, TX, 1976).
[2] W. Kohn and L. J. Sham, Phys. Rev. **140**, A1133 (1965).
[3] R. M. Martin, *Electronic Structure* (Cambridge University Press, New York, 2004).
[4] J. P. Perdew, V. N. Staroverov, J. Tao, and G. E. Scuseria, Phys. Rev. A **78**, 052513 (2008).
[5] J. P. Perdew and Y. Wang, Phys. Rev. B **45**, 13244 (1992).
[6] J. P. Perdew, K. Burke, and M. Ernzerhof, Phys. Rev. Lett. **77**, 3865 (1996); **78**, 1396 (1997).
[7] J. P. Perdew, A. Ruzsinszky, G. I. Csonka, O. A. Vydrov, G. E. Scuseria, L. A. Constantin, X. Zhou, and K. Burke, Phys. Rev. Lett. **100**, 136406 (2008); **102**, 039902 (2009).
[8] J. P. Perdew and Y. Wang, Phys. Rev. B **33**, 8800 (1986); **40**, 3399 (1989).
[9] J. P. Perdew, K. Burke, and Y. Wang, Phys. Rev. B **54**, 16533 (1996); **57**, 14999 (1998).
[10] J. Tao, J. P. Perdew, V. N. Staroverov, and G. E. Scuseria, Phys. Rev. Lett. **91**, 146401 (2003).
[11] J. P. Perdew, A. Ruzsinszky, G. I. Csonka, L. A. Constantin, and J. Sun, Phys. Rev. Lett. **103**, 026403 (2009).
[12] A. E. Mattsson, R. Armiento, and T. R. Mattsson, Phys. Rev. Lett. **101**, 239701 (2008).
[13] J. P. Perdew, A. Ruzsinszky, G. I. Csonka, O. A. Vydrov, G. E. Scuseria, L. A. Constantin, X. Zhou, and K. Burke, Phys. Rev. Lett. **101**, 239702 (2008).
[14] G. I. Csonka, O. A. Vydrov, G. E. Scuseria, A. Ruzsinszky, and J. P. Perdew, J. Chem. Phys. **126**, 244107 (2007).
[15] A. B. Alchagirov, J. P. Perdew, J. C. Boettger, R. C. Albers, and C. Fiolhais, Phys. Rev. B **63**, 224115 (2001).
[16] V. N. Staroverov, G. E. Scuseria, J. Tao, and J. P. Perdew, Phys. Rev. B **69**, 075102 (2004); **78**, 239907 (2008).
[17] G. I. Csonka, J. P. Perdew, A. Ruzsinszky, P. H. T. Philipsen, S. Lebegue, J. Paier, O. A. Vydrov, and J. G. Angyan, Phys. Rev. B **79**, 155107 (2009).
[18] P. Haas, F. Tran, and P. Blaha, Phys. Rev. B **79**, 085104 (2009); **79**, 209902 (2009).
[19] P. Haas, F. Tran, P. Blaha, L. S. Pedroza, A. J. R. da Silva, M. M. Odashima, and K. Capelle, Phys. Rev. B **81**, 125136 (2010).
[20] J. Sun, M. Marsman, A. Ruzsinszky, G. Kresse, and J. P. Perdew, Phys. Rev. B **83**, 121410 (2011).
[21] B. B. Karki, R. M. Wentzcovitch, S. de Gironcoli, and S. Baroni, Phys. Rev. B **61**, 8793 (2000).
[22] L. Schimka, J. Harl, and G. Kresse, J. Chem. Phys. **134**, 024116 (2011).
[23] J. Sun, M. Marsman, G. I. Csonka, A. Ruzsinszky, P. Hao, Y.-S. Kim, G. Kresse, and J. P. Perdew, Phys. Rev. B **84**, 035117 (2011).
[24] J. S. Dugdale and D. K. C. MacDonald, Phys. Rev. **89**, 832 (1953).
[25] P. Giannozzi, S. Baroni, N. Bonini, M. Calandra, R. Car, C. Cavazzoni, D. Ceresoli, G. L. Chiarotti, M. Cococcioni, I. Dabo *et al.*, J. Phys. Condens. Matter **21**, 395502 (2009).
[26] http://www.quantum-espresso.org (2010).
[27] S. Baroni, S. de Gironcoli, A. Dal Corso, and P. Giannozzi, Rev. Mod. Phys. **73**, 515 (2001).
[28] V. I. Ivashchenko and P. E. A. Turchi, Phys. Rev. B **78**, 224113 (2008).
[29] See Supplemental Material at http://link.aps.org/supplemental/10.1103/PhysRevB.85.014111 for experimental Debye temperature, lattice constants, and bulk moduli.
[30] G. teVelde and E. J. Baerends, Phys. Rev. B **44**, 7888 (1991).
[31] G. Wiesenekker and E. J. Baerends, J. Phys. Condens. Matter **3**, 6721 (1991).
[32] BAND2010, SCM, Theoretical Chemistry, Vrije Universiteit, Amsterdam, the Netherlands [http://www.scm.com].
[33] R. Neumann, R. H. Nobes, and N. C. Handy, Mol. Phys. **87**, 1 (1996).
[34] J. Tao, J. P. Perdew, and A. Ruzsinszky, Phys. Rev. B **81**, 233102 (2010).
[35] V. N. Staroverov, G. E. Scuseria, J. Tao, and J. P. Perdew, J. Chem. Phys. **119**, 12129 (2003).